

# Effect of friction on the hysteresis loops from three-point bending fatigue tests of fibre-reinforced composites

W. Van Paepegem<sup>a\*</sup>, K. De Geyter<sup>b</sup>, P. Vanhooymissen<sup>b</sup> and J. Degrieck<sup>a</sup>

<sup>a</sup> Professor, Dept. of Mechanical Construction and Production, Sint-Pietersnieuwstraat 41, 9000 Gent, Belgium

<sup>b</sup> Researcher, Dept. of Mechanical Construction and Production, Sint-Pietersnieuwstraat 41, 9000 Gent, Belgium

## Abstract

In uni-axial fatigue tests on fibre-reinforced composites, the stress-strain hysteresis loop can be used as a measure for stiffness degradation and energy dissipation. In case of three-point bending fatigue tests, the hysteresis loop of the bending force versus midspan displacement can yield similar information. In this paper, it is shown that the shape of the hysteresis loop can be affected significantly by friction at the supports, especially for large deflections. As such, the area of the closed hysteresis loop is no longer a measure for energy dissipation and damage growth.

Three-point bending fatigue tests have been compared to static bending tests with different support conditions. Finally finite element analyses have confirmed that friction can be identified as an important parameter affecting the shape of the hysteresis curve.

Keywords: fatigue, composites, bending experiments, friction

## 1. Introduction

The vast majority of fatigue tests on fibre-reinforced composites is performed in uni-axial tension/tension or tension/compression fatigue [1-5]. These tests are accepted by international standards (ASTM D3479) and provide the S-N data for the tested material.

Although bending fatigue tests are not widely accepted as a standard, they are used a lot for research purposes [6-8]. They do have some important advantages as well: (i) bending loads often occur in in-service loading conditions, (ii) there are no problems with buckling, compared to tension/compression fatigue, and (iii) the required forces are much smaller. To evaluate the stiffness degradation and damage growth in the fibre-reinforced laminate, the hysteresis loop of one loading cycle can be measured. In case of three-point bending fatigue, the history of bending force versus midspan displacement is recorded.

In this paper, it is shown that the friction between the tested material and the supports of the bending setup can significantly affect the shape of the measured hysteresis loop. As a consequence, the interpretation of measured hysteresis loops must be done very carefully. The area of the closed hysteresis loop is then not a direct representation for the energy dissipation and damage growth.

## 2. Testing procedures and Material

The apparatus was an Instron servohydraulic fatigue testing machine, equipped with a fixture for three-point bending. The two supports and the load striking edge at midspan all had a radius of 5 mm.

The dimensions of the experimental setup are schematically indicated in Figure 1.

---

\* Author to whom correspondence should be addressed ( E-mail : Wim.VanPaepegem@UGent.be ).

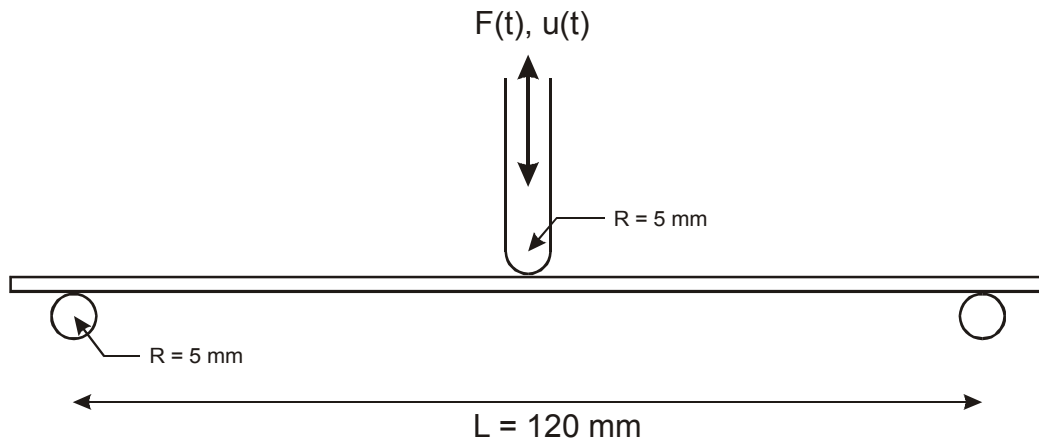


**Figure 1** Schematic representation of the bending fatigue setup.

Figure 2 shows the experimental setup.



**Figure 2** Picture of the bending fatigue setup.

The fibre-reinforced composite under study was a 5-harness satin weave carbon/PPS composite. Polyphenylene sulphide (PPS) is a commonly used thermoplastic matrix in aeronautical applications.

Eight layers of fabric were stacked in several stacking sequences:  $[0^\circ]_8$ ,  $[90^\circ]_8$ ,  $[0^\circ/90^\circ]_{2s}$ ,  $[90^\circ/0^\circ]_{2s}$  and  $[+45^\circ/-45^\circ]_{2s}$ . The angle indicates the warp direction of the reinforcement layer. The displacement amplitude varied between 12 and 15 millimetres. Due to this large deflection, the fatigue tests were displacement-controlled. Even at medium frequencies (1 – 3 Hz), the load control did not manage to impose these large displacement amplitudes.

### 3. Results

Figure 3 shows typical hysteresis loops of the bending force versus midspan deflection at several times during fatigue life for the  $[90^\circ/0^\circ]_{2s}$  carbon/PPS laminate. The amplitude of the midspan deflection was 14.5 mm and the testing frequency was 2.0 Hz. The hysteresis loops are gone through in clockwise direction (loading – unloading).

The problem treated in this paper, is the typical shape of the hysteresis curve.

Typical hysteresis curves in bending for  $[90^\circ/0^\circ]_{2s}$  carbon/PPS laminate

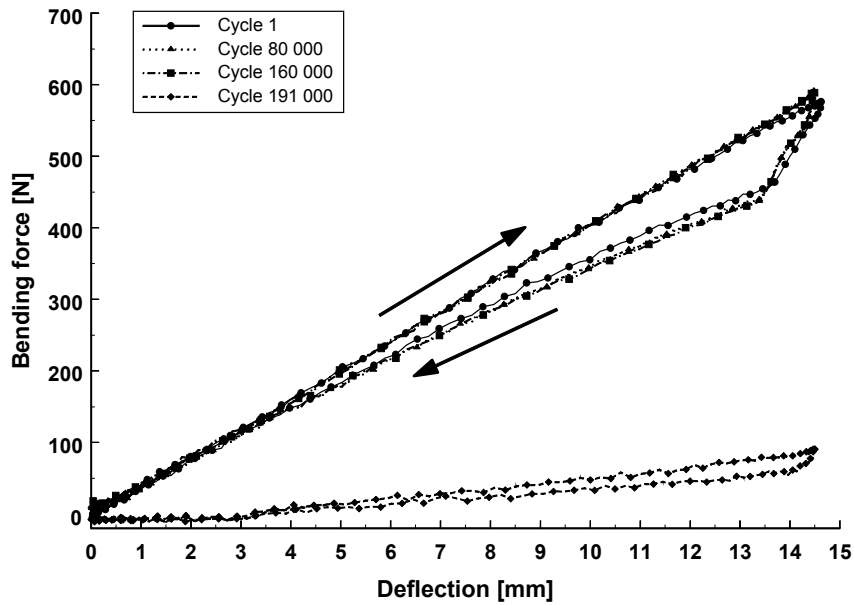
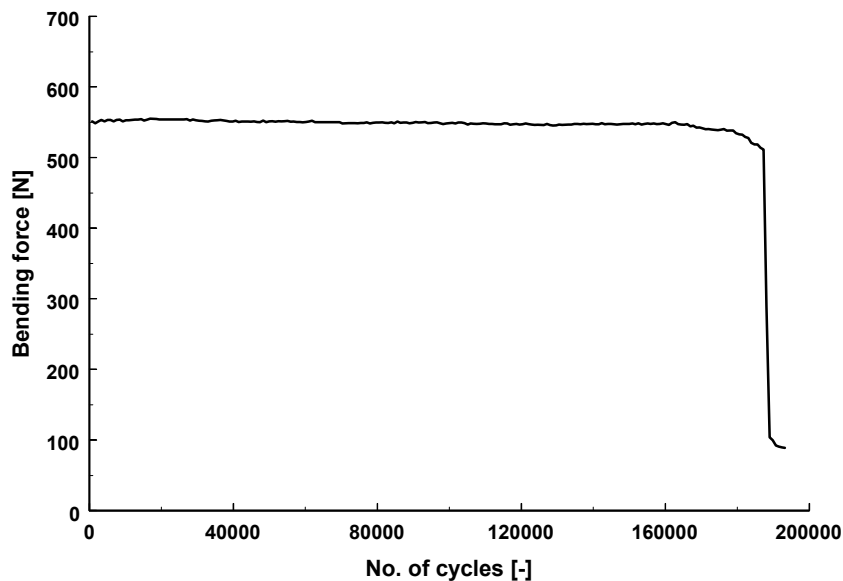


Figure 3 Typical hysteresis curves in bending for  $[90^\circ/0^\circ]_{2s}$  carbon/PPS laminate.

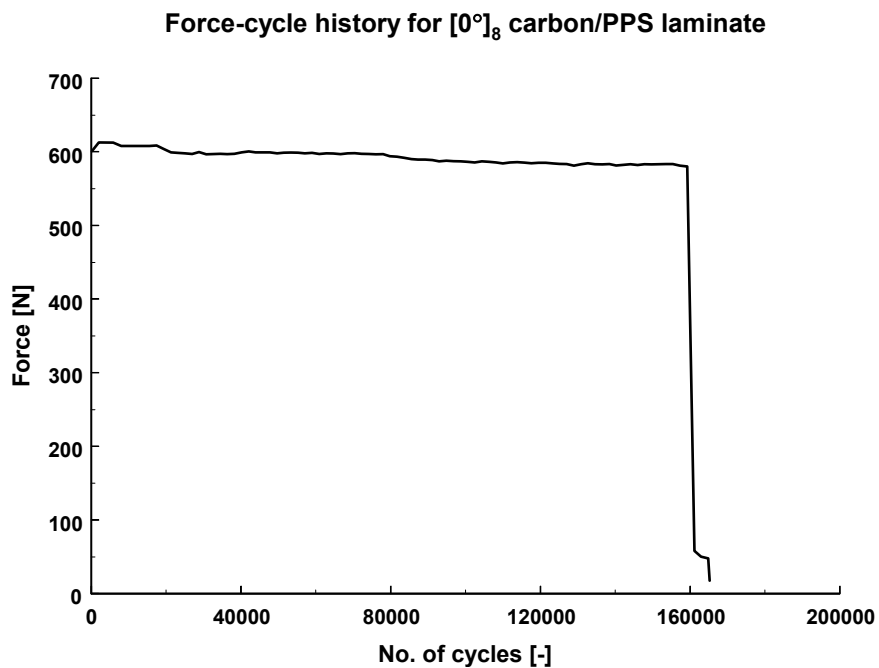
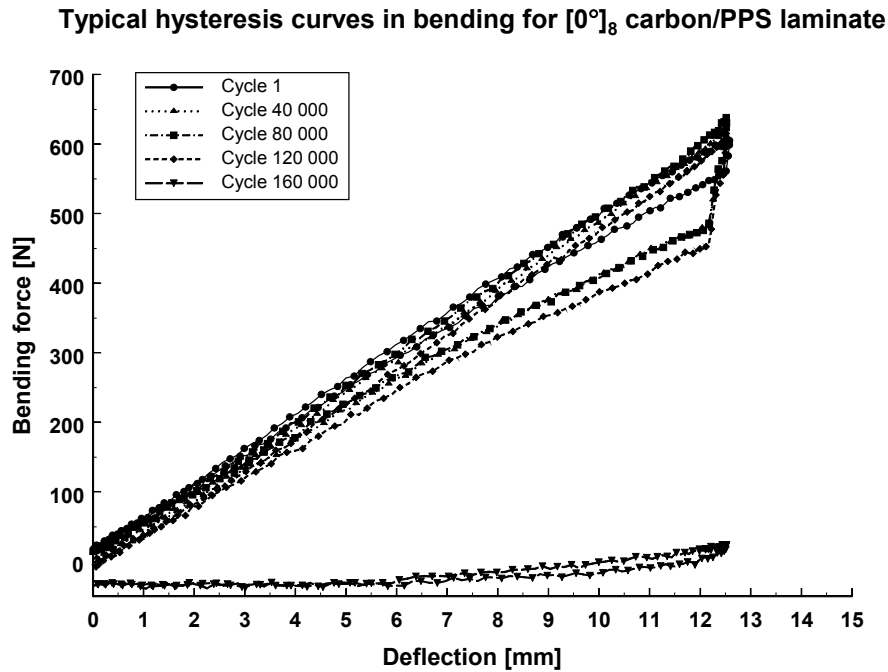
Figure 4 shows the corresponding force-cycle history for the  $[90^\circ/0^\circ]_{2s}$  laminate, with the force being the first harmonic amplitude of the recorded force waveform.

Force-cycle history for  $[90^\circ/0^\circ]_{2s}$  carbon/PPS laminate



**Figure 4** Force-cycle history for  $[90^{\circ}/0^{\circ}]_2$  carbon/PPS laminate.

The shape of the hysteresis loop does not depend on the stacking sequence of the laminate. Figure 5 and Figure 6 show the hysteresis curves and corresponding force-cycle history for a  $[0^{\circ}]_8$  laminate. The amplitude of the midspan deflection was 12.5 mm and the testing frequency was 2.0 Hz.



What does affect the shape of the hysteresis loop, is the magnitude of the deflection, but that is expected anyway, because a larger deflection would cause more fatigue damage than a smaller one.

Figure 7 shows the force-displacement curve for a set of triangular displacement waveforms with different amplitude. For a midspan deflection of 17 mm, the shape of the hysteresis curve is found again. The displacement speed was 200 mm/min.

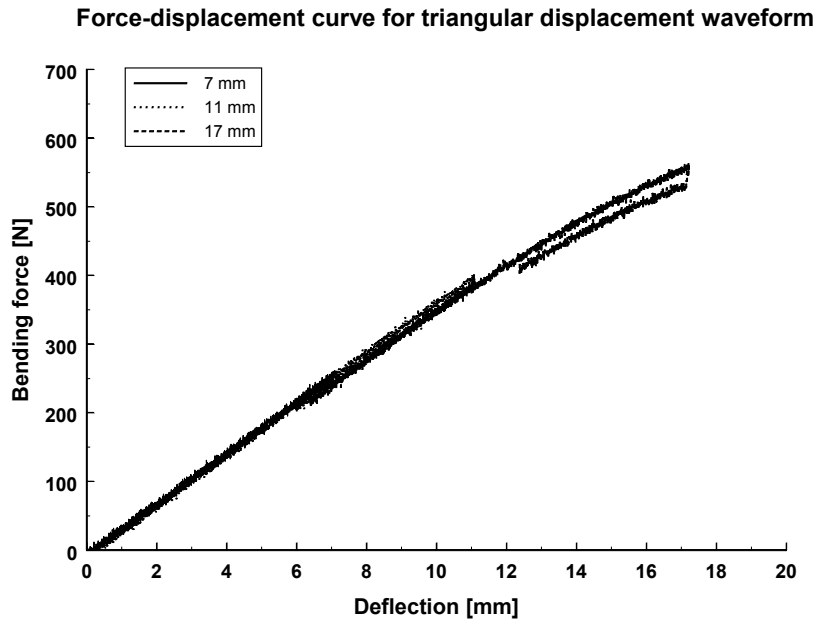


**Figure 7** Force-displacement curve of  $[90^{\circ}/0^{\circ}]_{2s}$  carbon/PPS laminate for triangular displacement waveforms with increasing amplitude.

For the midspan deflection of 17 mm, Figure 8 shows the time history of the bending force and the displacement. It is important to notice the sudden drop in the bending force at the transition from loading to unloading.

**Time history of force and displacement for triangular displacement waveform**

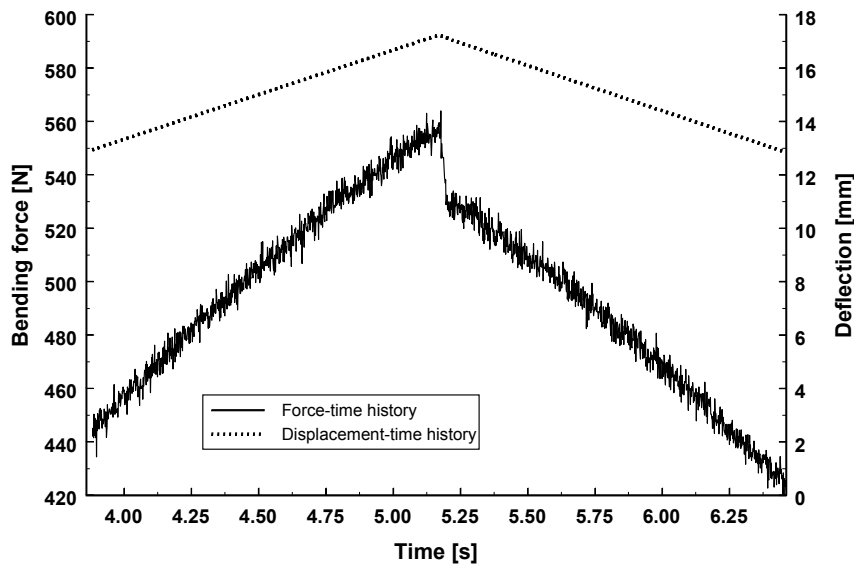


**Figure 8** Time history of force and displacement of  $[90^{\circ}/0^{\circ}]_{2s}$  carbon/PPS laminate for triangular displacement waveforms with 17.0 mm amplitude.

To assess the contribution of inertia effects and the importance of supporting conditions, the experiments were repeated under static loading conditions (displacement speed 2 mm/min). The specimens were now instrumented with a strain gauge that measures the longitudinal tensile strain at midspan.

Due to the limited deformation of the strain gauge, the deflection was restricted to 10.0 mm. Three different support conditions were tested: (i) contact specimen-Teflon sheet, (ii) contact specimen-bare steel, and (iii) contact specimen-emery paper. Figure 9 shows the measured curves of bending force versus midspan deflection. The shape of the hysteresis curve can be varied by varying the friction at the end supports. The effect is less pronounced due to the smaller deflection.

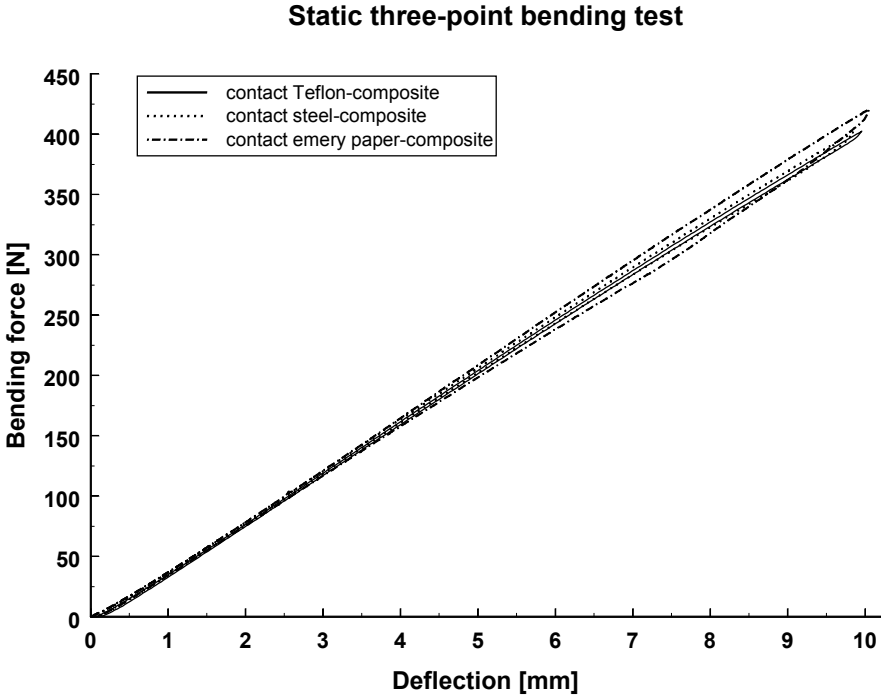


Figure 9 Static force-displacement curve of  $[90^{\circ}/0^{\circ}]_{2s}$  carbon/PPS laminate with different support conditions: (i) Teflon, (ii) steel and (iii) emery paper.

Figure 10 shows the corresponding curve of the bending force versus strain gauge measurement.

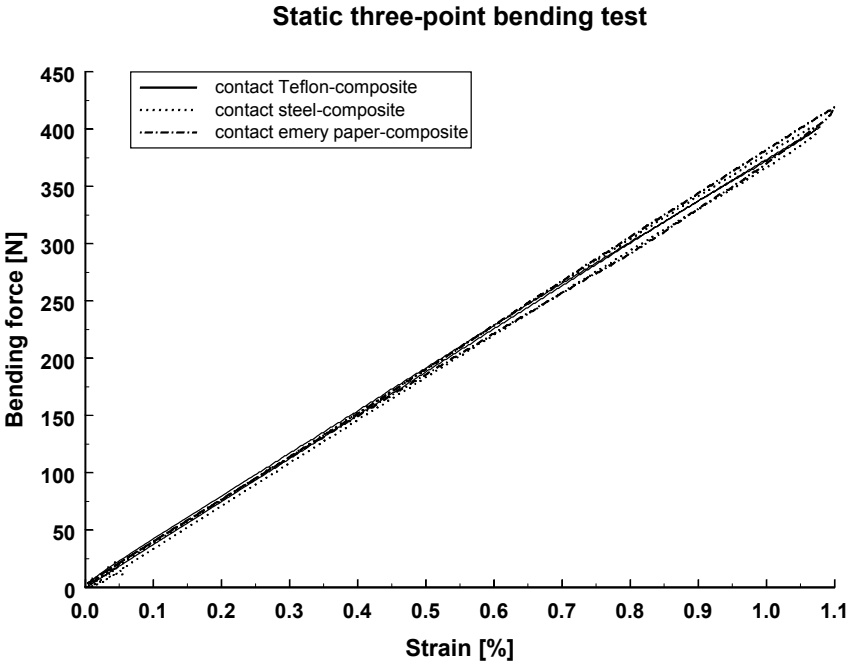
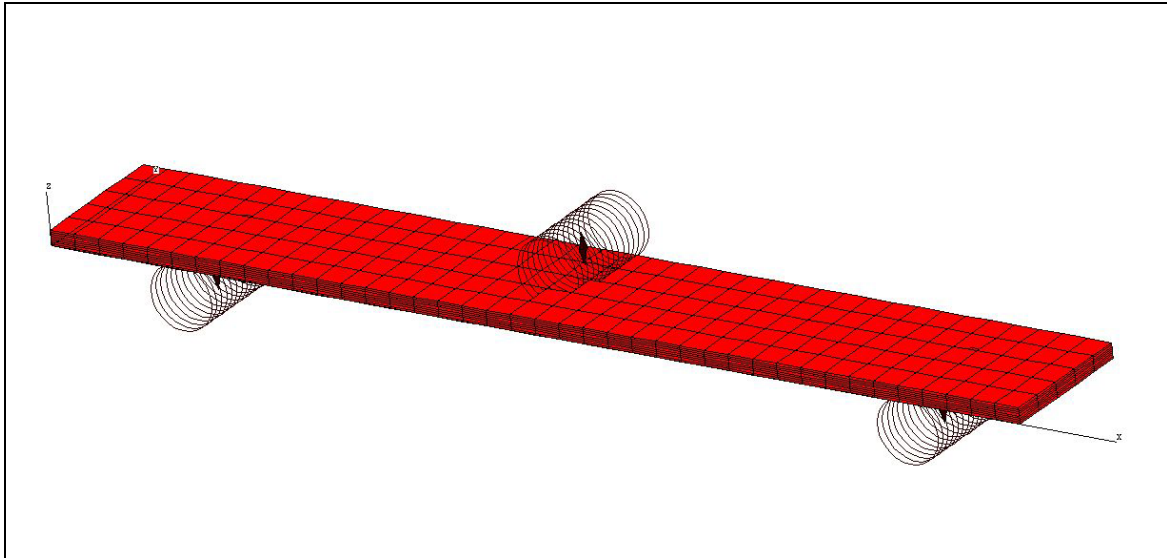


Figure 10 Bending force versus midspan tensile strain of  $[90^{\circ}/0^{\circ}]_{2s}$  carbon/PPS laminate with different support conditions: (i) Teflon, (ii) steel and (iii) emery paper.

Finally finite element simulations have been done to prove the hypothesis of friction affecting the shape of the hysteresis loop.

The simulations have been done with the commercial implicit finite element code SAMCEF™. The finite element mesh is shown in Figure 11. Eight layers of composite have been modelled with isoparametric volumic elements, one element per layer through the thickness. The end supports and the load striking edge have been modelled as rigid body cylinders with radius 5 mm. The contact conditions between supports and composite elements can have a different friction coefficient.

The material is assumed to behave in a linear elastic manner, but the geometric nonlinearity is taken into account.



**Figure 11** SAMCEF™ finite element model of the three-point bending test.

Figure 12 shows the simulated deflection of the  $[90^{\circ}/0^{\circ}]_{2s}$  specimen for a prescribed midspan displacement of 14.5 mm (in agreement with the imposed displacement in the three-point bending fatigue tests).

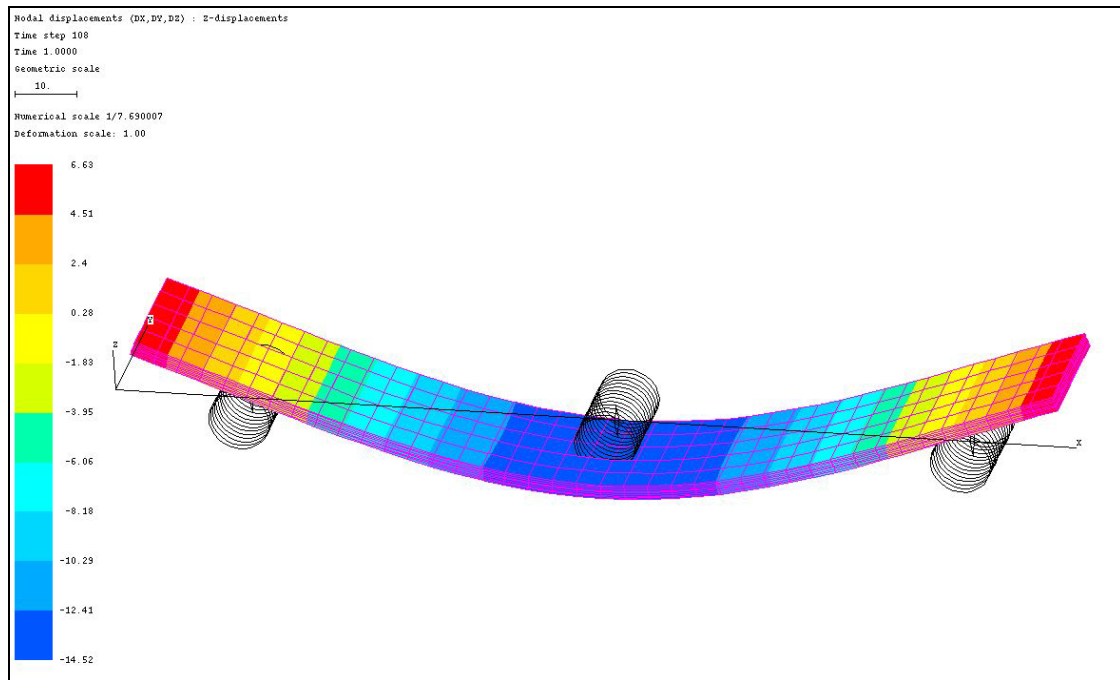


**Figure 12** Simulated displacement contours for a three-point bending test on a  $[90^\circ/0^\circ]_{2s}$  carbon/PPS laminate.

In Figure 13, the simulated hysteresis curves are plotted for different friction conditions. The complete loading-unloading path has been simulated, where the imposed midspan displacement increases from 0.0 to 14.5 mm and decreases back to 0.0 mm. The curve of bending force versus midspan deflection is shown for four different friction conditions at the two end supports: (i)  $\mu = 0.0$ , (ii)  $\mu = 0.1$ , (iii)  $\mu = 0.2$  and (iv)  $\mu = 0.3$ .

It can be clearly seen that for  $\mu = 0.0$ , there is no hysteresis. However, the curve is slightly nonlinear due to the geometric nonlinearity (large deflection). For  $\mu = 0.3$ , the typical shape of the hysteresis curve is found back, although no material damage was taken into account. As a consequence, the shape variation is only due to the friction coefficient.

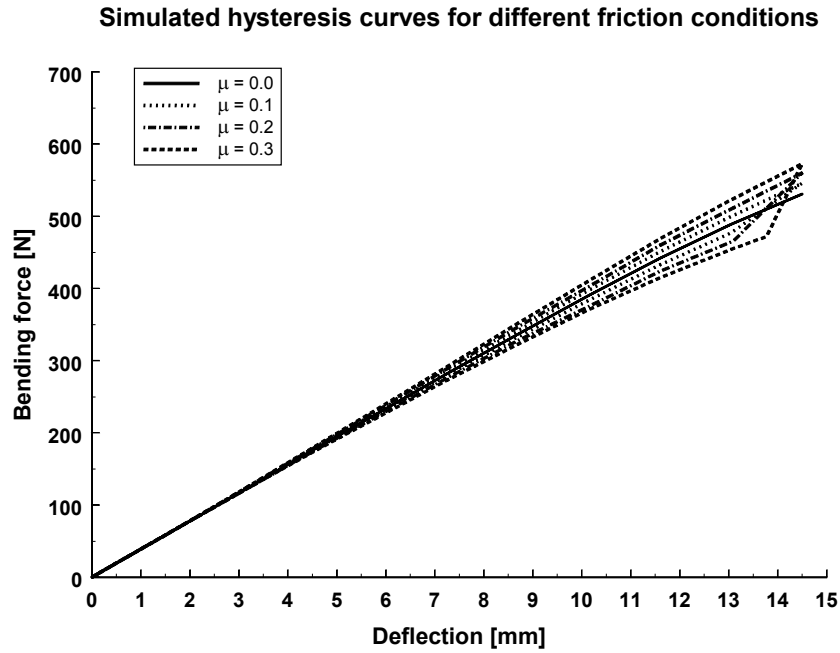


**Figure 13** Simulated hysteresis curves for a  $[90^{\circ}/0^{\circ}]_{2s}$  carbon/PPS laminate with different friction conditions at the supports: (i)  $\mu = 0.0$ , (ii)  $\mu = 0.1$ , (iii)  $\mu = 0.2$  and (iv)  $\mu = 0.3$ .

The simulation for  $\mu = 0.3$  has been done again with a very small time step at the transition from loading to unloading. The effect is even more pronounced, as can be seen in Figure 14. It is worth to mention that the value of the maximum bending force is in very good agreement with the experimentally measured one during the three-point bending fatigue tests (see Figure 3 and Figure 4).

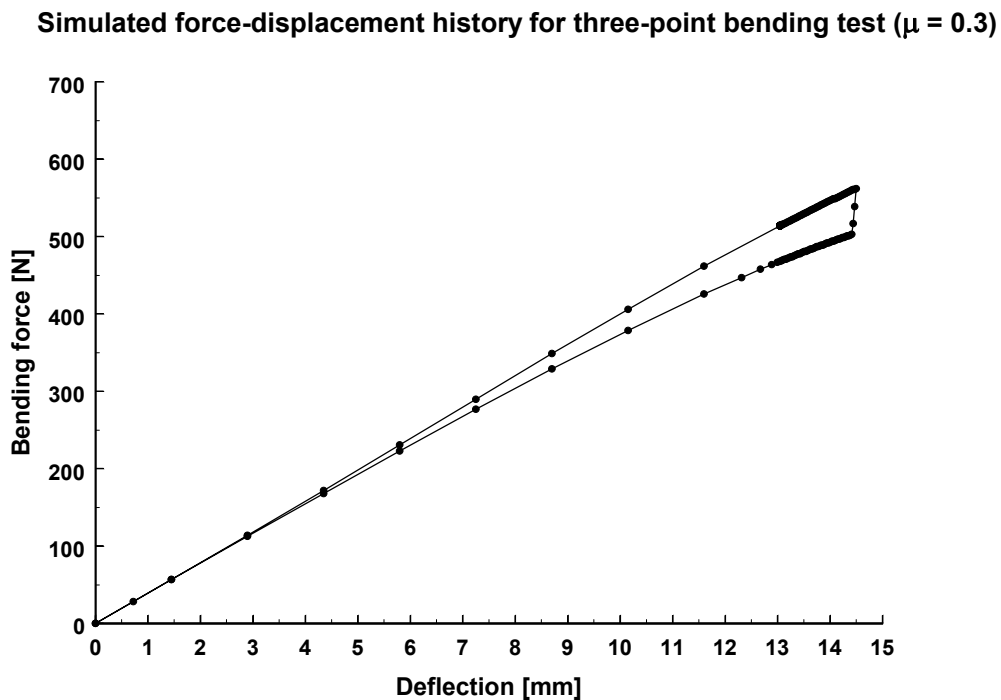


**Figure 14** Detailed simulation of the force-displacement curve of the  $[90^\circ/0^\circ]_{2s}$  carbon/PPS laminate for  $\mu = 0.3$ .

In Figure 15, the simulated bending force has been plotted versus the simulated longitudinal tensile strain  $\varepsilon_{11}$  in a volumic element near the middle of the span. The hysteresis loop can be recovered, in qualitative agreement with the strain gauge instrumented static bending test (see Figure 10).

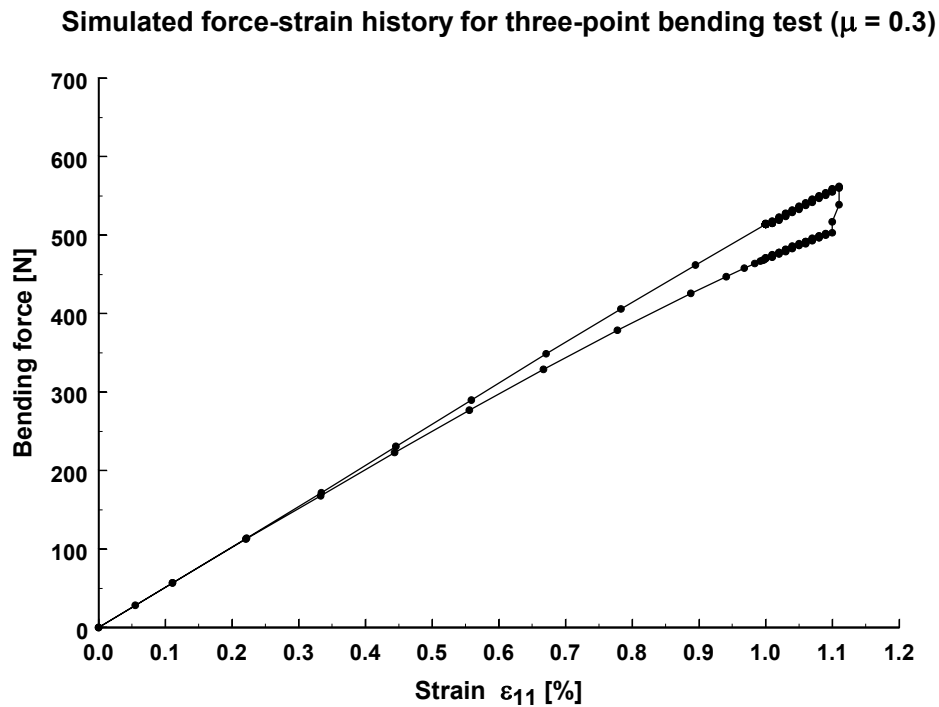


**Figure 15** Simulated bending force vs. longitudinal tensile strain of  $[90^\circ/0^\circ]_{2s}$  carbon/PPS laminate for  $\mu = 0.3$ .

Finally, the simulated stress-strain history for that same volumic element in Figure 16 proves that there is no material hysteresis.

### Simulated stress-strain history for three-point bending test ( $\mu = 0.3$ )

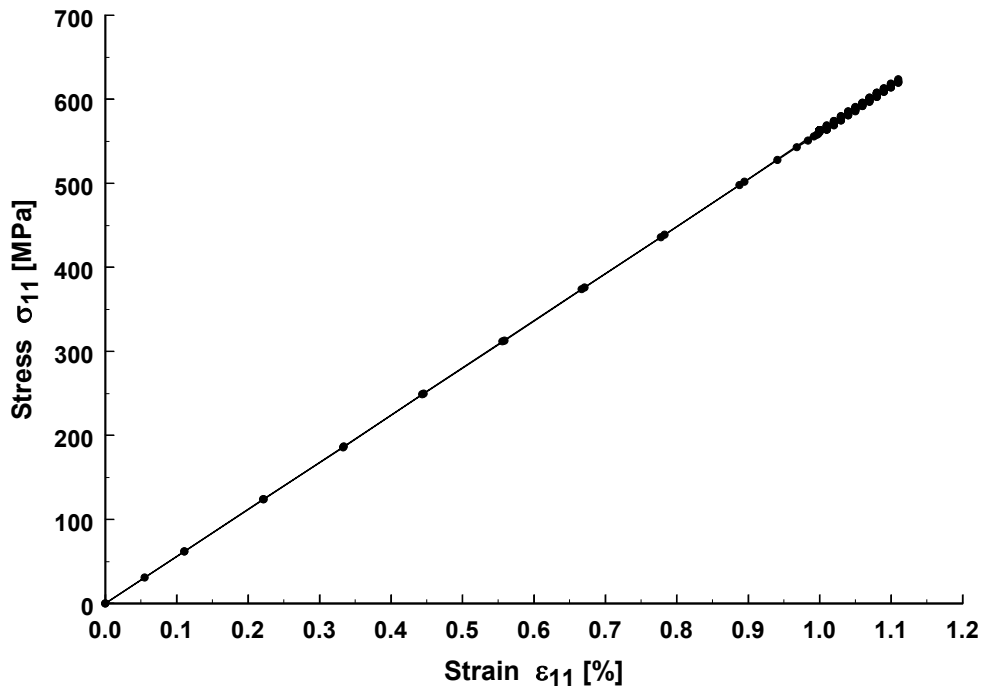


Figure 16 Simulated stress-strain history of  $[90^{\circ}/0^{\circ}]_2$  carbon/PPS laminate for  $\mu = 0.3$ .

## 4. Conclusions

Hysteresis loops of bending force versus midspan deflection were recorded from three-point bending fatigue tests on fibre-reinforced composites. A typical shape of the hysteresis curves could be detected, independent of material characteristics.

In this paper, it was shown that the friction between the composite specimen and the supports was the predominant cause of this phenomenon. Static bending tests with different support conditions were performed and three-dimensional finite element analyses were done with different friction coefficients. These tests confirmed the hypothesis.

Therefore, it can be concluded that the information from hysteresis loops in bending must be considered very carefully. Although stiffness degradation and micromechanical damage growth are typical fatigue mechanisms for fibre-reinforced composites, they cannot be directly related with the recorded force-displacement hysteresis curve of three-point bending tests.

## Acknowledgements

The author W. Van Paepegem gratefully acknowledges his finance through a grant of the Fund for Scientific Research – Flanders (F.W.O.).

The authors also express their gratitude to Syncoglas for their support and technical collaboration.

## References

- [1] Hansen, U. (1999). Damage development in woven fabric composites during tension-tension fatigue. *Journal of Composite Materials*, 33(7), 614-639.
- [2] Coats, T.W. and Harris, C.E. (1995). Experimental verification of a progressive damage model for IM7/5260 laminates subjected to tension-tension fatigue. *Journal of Composite Materials*, 29(3), 280-305.
- [3] Caprino, G. (2000). Predicting fatigue life of composite laminates subjected to tension-tension fatigue. *Journal of Composite Materials*, 34(16), 1334-1355.
- [4] Gamstedt, E.K. and Sjogren, B.A. (1999). Micromechanisms in tension-compression fatigue of composite laminates containing transverse plies. *Composites Science and Technology*, 59(2), 167-178.
- [5] Rotem, A. (1991). The fatigue behaviour of orthotropic laminates under tension-compression loading. *International Journal of Fatigue*, 13(3), 209-215.
- [6] Sedrakian, A., Ben Zineb, T., Billoet, J.L., Sicot, N. and Lardeur, P. (1997). A numerical model of fatigue behaviour for composite plates: application to a three point bending test. In : Degallaix, S., Bathias, C. and Fougères, R. (eds.). *International Conference on fatigue of composites. Proceedings, 3-5 June 1997, Paris, France, La Société Française de Métallurgie et de Matériaux*, pp. 415-423.
- [7] Sidoroff, F. and Subagio, B. (1987). Fatigue damage modelling of composite materials from bending tests. In : Matthews, F.L., Buskell, N.C.R., Hodgkinson, J.M. and Morton, J. (eds.). *Sixth International Conference on Composite Materials (ICCM-VI) & Second European Conference on Composite Materials (ECCM-II) : Volume 4. Proceedings, 20-24 July 1987, London, UK, Elsevier*, pp. 4.32-4.39.
- [8] Caprino, G. and D'Amore, A. (1998). Flexural fatigue behaviour of random continuous-fibre-reinforced thermoplastic composites. *Composites Science and Technology*, 58, 957-965.
- [9] Shackelford, J.F., Alexander, W. and Park, J.S. (1995). *Practical handbook of materials selection*. Boca Raton, Florida, CRC Press, 625 pp.
- [10] Kalpakjian, S. (1992). *Manufacturing Engineering and Technology*. Reading, Massachusetts, Addison-Wesley Publishing Company, 1258 pp.
- [11] Avallone, E.A. and Baumeister, T. (1996). *Marks' Standard Handbook for Mechanical Engineers*. New York, McGraw-Hill.